

Effect of the catalyst supports on the removal of perchloroethylene (PCE) over chromium oxide catalysts

Sung Dae Yim, Dong Jun Koh, In-Sik Nam* and Young Gul Kim

Research Center for Catalytic Technology (RCCT), Department of Chemical Engineering, School of Environmental Engineering,
Pohang University of Science and Technology (POSTECH)/Research Institute of Industrial Science and Technology (RIST),
San 31 Hyoja-Dong, Pohang 790-784, Korea
E-mail: isnam@postech.ac.kr

Received 9 August 1999; accepted 2 December 1999

The oxidation of perchloroethylene (PCE) was investigated over chromium oxide catalysts supported on TiO_2 , Al_2O_3 , SiO_2 , SiO_2 – Al_2O_3 and activated carbon. The phase of chromium oxide on the catalyst surface is critical for the oxidation of PCE. The catalytic activity of PCE removal enhances as the formation of Cr(VI) species on the catalyst surface increases. The surface area and the type of the catalyst supports were also essential for high performance in the PCE oxidation. In addition, the structure of Cr(VI) on the catalyst surface also plays an important role for the decomposition of PCE. The polymerized Cr(VI) mainly formed by the interaction of metals with the support is the active reaction site for the present reaction system. $\text{CrO}_x/\text{TiO}_2$ reveals the strongest PCE removal activity among the catalysts examined in the present study.

Keywords: chlorinated hydrocarbons, chromia, titania, alumina, CVOCs, oxidation

1. Introduction

Chlorinated volatile organic compounds (CVOCs) such as trichloroethylene (TCE), perchloroethylene (PCE), and methylene chloride, which are known to be hazardous to humans, are recognized as precursors for the formation of ground-level ozone and photochemical smog in urban areas. Among the emission control technologies for CVOCs, catalytic oxidation has been widely employed because of the mild operating conditions, low energy consumption and less formation of noxious by-products.

There have been a number of investigations on the catalytic oxidation of CVOCs over various metal and metal oxide catalysts [1–15]. Bond and Sadeghi [2] studied a platinum catalyst supported on a γ -alumina for the complete oxidation of methylene chloride, methyl chloride, carbon tetrachloride, dichloroethylene, trichloroethylene and perchloroethylene. Lou and Lee [3] also investigated the oxidation of trichloromethane over a $\text{Pt}/\text{Al}_2\text{O}_3$ alloy catalyst. Manning [4] examined a commercial 12.5 wt% $\text{Cr}_2\text{O}_3/\text{Al}_2\text{O}_3$ fluid bed catalyst for the oxidation of methylene chloride and three other chlorinated ethylenes. A hopcalite catalyst was employed for the purification of air containing 19 halogenated hydrocarbons [5]. Cation-exchanged zeolite Y catalysts such as HY, CrY, CeY [6], $\text{TiO}_2/\text{SiO}_2$ acid catalyst [7], chromium trioxide supported on porous carbon [8], and chromium-doped alumina pillared clay [9] have been also reported to be promising for the oxidation of CVOCs.

In an earlier study, the oxidation of trichloroethylene (TCE) was investigated over supported platinum and vari-

ous transition metal oxides catalysts with 1 wt% metal content in a fixed-bed flow reactor system [10]. When Pt was impregnated on the various types of catalyst supports, TiO_2 exhibited the best performance. Over the TiO_2 -supported catalysts, the oxidation activity depended on the types of metals, and the TCE removal activity increased in the order of CrO_x (98%) > MnO_x (79%) > Pt (72%) > CoO_x \approx CuO_x (58%) > FeO_x (54%) > NiO_x (49%) at 400 °C. Therefore, $\text{CrO}_x/\text{TiO}_2$ seems to be the most effective catalyst for the oxidation of TCE under the experimental conditions covered in the previous study [10]. The supported chromium oxide catalysts have been already reported to be very active for the oxidation of CVOCs [1,4,6,8–13]. Especially, the alumina-supported 12.5 wt% chromium oxide catalyst has been widely employed as a commercial CVOCs removal catalyst [4,12]. However, a systematic study examining the role of catalyst support for catalytic removal of CVOCs can hardly be found.

The activity of CrO_x supported on TiO_2 , Al_2O_3 , SiO_2 – Al_2O_3 , SiO_2 and activated carbon containing 12.5 wt% of Cr was examined in a fixed-bed flow reactor for the removal of perchloroethylene (PCE) as a standard compound of CVOCs. On the basis of the catalytic performance and catalyst characterization with XRD, XPS, NH_3 TPD, TPR and Raman, the catalyst was optimized for the removal of PCE by the identification of the active reaction sites on the catalyst surface.

2. Experimental

The supported chromium oxide catalysts were prepared by the incipient wetness impregnation method with an aque-

* To whom correspondence should be addressed.

ous solution of chromium nitrate ($\text{Cr}(\text{NO}_3)_3 \cdot 9\text{H}_2\text{O}$, Aldrich Chemical Co.). The supports employed in the present study were TiO_2 (Hombikat UV-100, 250 m^2/g ; Degussa P-25, 58 m^2/g ; Shinyo, 17 m^2/g), Al_2O_3 (Aldrich, 290 and 155 m^2/g ; Norton, 25 m^2/g), $\text{SiO}_2\text{-Al}_2\text{O}_3$ (JRC-SAL-2, 560 m^2/g), SiO_2 (Cab-O-Sil, 300 m^2/g) and activated carbon (Aldrich, 850 m^2/g). After the impregnation of CrO_x on the supports, the catalysts were subsequently dried at 110 °C for 12 h, and calcined in air at 450 °C for 5 h. Note that CrO_x /activated carbon was calcined in air at 350 °C for 5 h to avoid the oxidation of carbon.

The oxidation of PCE was carried out in a fixed-bed continuous-flow reactor. The reactor is a 6 mm o.d. Pyrex glass tube operated in the mode of down flow. A reactant mainly containing air with 30 ppm of PCE was fed into the reactor charging 60/80 mesh size catalyst at a flow rate of 600 ml/min, equivalent to a reactor space velocity of 30,000 h^{-1} . The reaction temperatures were varied from 150 to 350 °C under atmospheric pressure. The feed and product streams of the reactor were analyzed by on-line HP 5890 gas chromatography (GC) with TCD and FID detectors. The conversion of PCE was calculated based upon the difference between inlet and outlet concentrations of PCE. No chlorinated by-products were detected in the down stream of the reactor during the course of reaction. The other products such as HCl and Cl_2 were not analyzed due to the low concentration in the product stream. However, it has been examined that more than 90% of PCE converted to CO and CO_2 by carbon balance. In addition, no residues of chlorinated and carbon compounds were found on the catalyst surface after reaction by the surface titration with XPS, AA and ion chromatography.

X-ray powder diffraction patterns of the catalyst prepared in the present study were observed by an M18XHF (MAC Science Co.) diffractometer employing $\text{Cu K}\alpha$ radiation ($\lambda = 1.5405 \text{ \AA}$). Quantitative X-ray diffraction data were obtained by comparing the intensity ratio of Cr_2O_3 [110]/ Al_2O_3 [440] and Cr_2O_3 [110]/ TiO_2 [101] examined for the samples of the catalysts with respect to the mixing ratios of pure Cr_2O_3 , Al_2O_3 and TiO_2 . The specific surface areas were determined by BET apparatus from Micromeritics (ASAP 2010C).

XPS data were obtained by KRATOS Analytical XSAM 800 cpi ESCA equipped with a Mg anode (Mg $\text{K}\alpha$ radiation, 1253.6 eV) and spherical analyzer operating at 15 kV and 15 mA. Binding energies for the catalyst samples were referenced to the C 1s line (284.6 eV) of the carbon overlayer. The oxidation state of chromium distributed on the catalyst surface was determined by nonlinear least-squares curve fitting using the Cr $2p_{3/2}$ envelope. In order to minimize the photoreduction of chromium oxide species on the catalyst surface during XPS experiments, all the catalyst samples were analyzed within the short period of time less than 20 min [16].

Temperature-programmed reduction (TPR) experiments were carried out using 50 mg of the catalysts under hydrogen (5%) in the flow of nitrogen with 40 ml/min heated

at 10 °C/min. The catalysts were pre-treated with oxygen at 500 °C for 0.5 h. A thermal conductivity detector (HP 5890 GC) was employed to monitor the consumption of hydrogen during the reduction of the catalyst.

Raman spectra were recorded from powdered samples pressed into self-supporting wafers. The spectra were obtained in the 180° configuration on a 532-RENS-A01 model, using the 514.5 nm radiation of argon ion gas as an excitation source. The laser power at the sample wafers was 25 mW, and the spectral resolution was 3–4 cm^{-1} . The scattered radiation was detected by Wright instruments with an intensified photodiode array cooled thermoelectrically to –30 °C. The Raman spectra were obtained at room temperature and under ambient conditions.

3. Results and discussion

Figure 1 shows the PCE removal activity of 12.5 wt% CrO_x catalysts supported on Al_2O_3 (290 m^2/g), $\text{SiO}_2\text{-Al}_2\text{O}_3$, TiO_2 (58 m^2/g), SiO_2 and activated carbon. The removal activity strongly depended on the types of support. It increased in the following order: Al_2O_3 (90.0%) > $\text{SiO}_2\text{-Al}_2\text{O}_3$ (65.0%) > TiO_2 (57.3%) > SiO_2 (18.9%) > activated carbon (12.0%) at 200 °C. It is probably due to the alteration of morphology of chromium oxide on the catalyst surface, which was also investigated by Kim et al. [17] for the partial oxidation of alcohol over a CrO_x catalyst. It should be noted that 12.5 wt% of Cr is the optimal content on the catalyst surface. The PCE removal activity of the catalysts examined in the present study improved as the content of Cr increased up to 12.5 wt%. The commercial $\text{Cr}_2\text{O}_3/\text{Al}_2\text{O}_3$ catalyst also contains a similar Cr content. Since no deactivation of the catalyst was observed during the course of reaction up to 100 h of on-stream time, the evaporation of CrO_x on the catalyst surface may not occur under the reaction conditions covered in the present study.

Based upon XRD patterns shown in figure 2, the intensities of the crystalline $\alpha\text{-Cr}_2\text{O}_3$ peaks decrease as the PCE

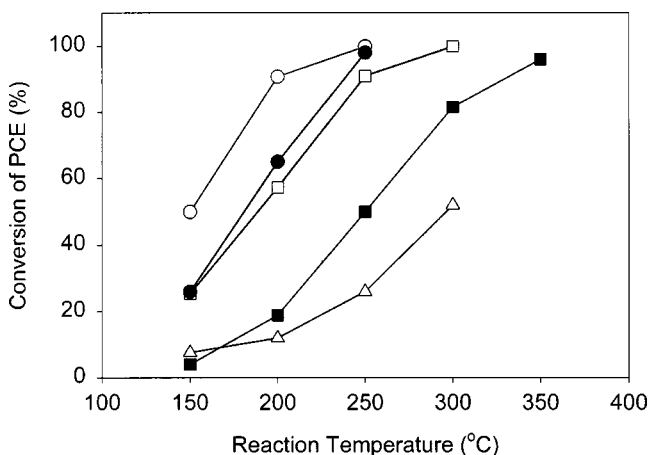


Figure 1. PCE removal activity over 12.5 wt% CrO_x catalysts supported on Al_2O_3 (290 m^2/g) (○), $\text{SiO}_2\text{-Al}_2\text{O}_3$ (●), TiO_2 (58 m^2/g) (□), SiO_2 (■) and activated carbon (△).

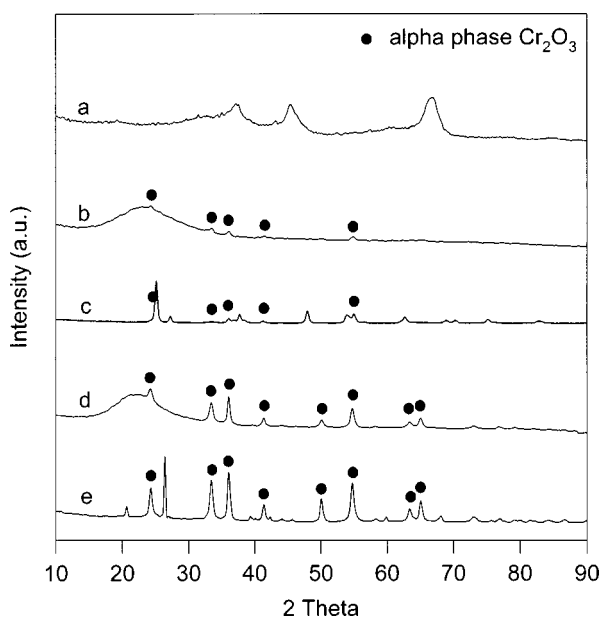


Figure 2. X-ray diffraction patterns of CrO_x catalysts supported on Al_2O_3 (290 m^2/g) (a), $\text{SiO}_2\text{-Al}_2\text{O}_3$ (b), TiO_2 (58 m^2/g) (c), SiO_2 (d) and activated carbon (e).

removal activity increases, and no $\alpha\text{-Cr}_2\text{O}_3$ peak can be found for the most active catalyst for the removal of PCE, $\text{CrO}_x/\text{Al}_2\text{O}_3$. The results from XRD were quite consistent with XPS studies of 12.5 wt% CrO_x catalysts which shows the increase of the number of Cr(III) species on the catalyst surface as the formation of $\alpha\text{-Cr}_2\text{O}_3$ increases. Therefore, crystalline $\alpha\text{-Cr}_2\text{O}_3$ may not be the active reaction sites on the chromia catalyst for the present reaction system.

It is generally recognized that the formation of crystalline $\alpha\text{-Cr}_2\text{O}_3$ phase has been reduced on the surface of TiO_2 and Al_2O_3 due to the strong interaction of TiO_2 and Al_2O_3 with chromium oxide [18,19]. However, the XRD pattern of the 12.5 wt% $\text{CrO}_x/\text{TiO}_2$ catalyst reveals the phase for crystalline $\alpha\text{-Cr}_2\text{O}_3$, while that of $\text{CrO}_x/\text{Al}_2\text{O}_3$ cannot be observed, as shown in figure 2. This strongly implies that the surface area of the catalysts, particularly for CrO_x catalysts with high loadings of Cr, can play a critical role in the formation of the active phase of CrO_x on the catalyst surface for the high performance of PCE decomposition. The $\alpha\text{-Cr}_2\text{O}_3$ will more easily form on the surface of TiO_2 (58 m^2/g) due to the low capacity of the monolayer coverage of Cr loadings than on the high surface area of Al_2O_3 (290 m^2/g) as Cr loadings increase. Previous studies have also discussed that the surface of the catalyst support becomes saturated with the surface chromium oxide up to the critical metal loading for the formation of a monolayer of Cr, and the additional Cr leads to the formation of crystalline $\alpha\text{-Cr}_2\text{O}_3$ on the catalyst surface [20–22]. Therefore, it is expected that CrO_x catalysts supported on the high surface area of TiO_2 may form little $\alpha\text{-Cr}_2\text{O}_3$, and reveal high removal activity of PCE.

To investigate the effect of surface area of TiO_2 and Al_2O_3 which reveals the high performance of PCE removal, 12.5 wt% CrO_x catalysts supported on TiO_2 (17, 58 and

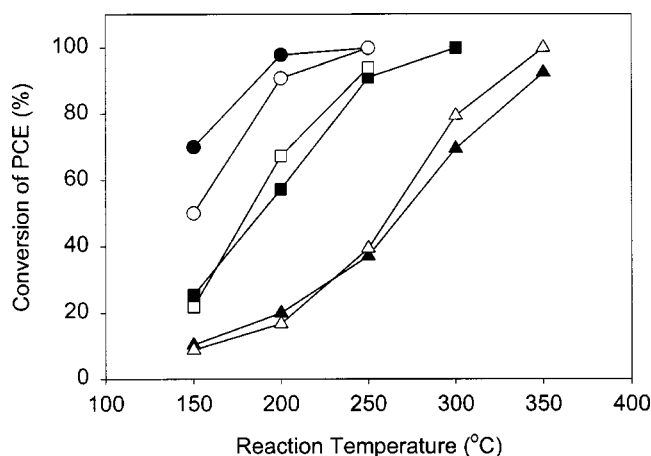


Figure 3. PCE removal activity over 12.5 wt% CrO_x catalysts supported on TiO_2 (250 m^2/g) (●), 58 m^2/g (■) and 17 m^2/g (▲) and Al_2O_3 (290 m^2/g) (○), 155 m^2/g (□) and 25 m^2/g (Δ).

250 m^2/g) and Al_2O_3 (25, 155 and 290 m^2/g) with a variety of catalyst surface areas were examined and are given in figure 3. As the surface area of TiO_2 and Al_2O_3 increases, the removal activity of PCE also proportionally increases. Furthermore, with a similar surface area of both catalysts, TiO_2 exhibits higher PCE removal activity at the given content of Cr on the catalyst surface. Therefore, $\text{CrO}_x/\text{TiO}_2$ (250 m^2/g) shows the highest catalytic activity among the catalysts examined in the present study for the oxidation of PCE. Note that a reason for the highest activity of $\text{CrO}_x/\text{Al}_2\text{O}_3$ commonly employed as a CVOCs removal catalyst is mainly the high surface area and easy availability of Al_2O_3 .

Figure 4 shows XRD patterns of 12.5 wt% $\text{CrO}_x/\text{TiO}_2$ and Al_2O_3 catalysts containing a variety of surface areas. The intensities of the $\alpha\text{-Cr}_2\text{O}_3$ peaks decreased as the surface area of TiO_2 and Al_2O_3 increases, and no $\alpha\text{-Cr}_2\text{O}_3$ XRD peaks can be found for high surface area of TiO_2 (250 m^2/g) and Al_2O_3 (290 m^2/g). As listed in table 1, the quantitative XRD measurements indicate that the amount of $\alpha\text{-Cr}_2\text{O}_3$ on the catalyst surface varies from 0 to 5.86 wt% and from 0 to 7.33 wt% with respect to the variation of the surface area of TiO_2 , and Al_2O_3 from 17 to 250 m^2/g and from 25 to 290 m^2/g , respectively. The relationship between the surface area of supports and the content of $\alpha\text{-Cr}_2\text{O}_3$ on the catalyst surface well agrees with the dependence of PCE removal activity on the surface area of the catalysts. It is basically due to the formation of less active $\alpha\text{-Cr}_2\text{O}_3$ on the catalyst surface for the present reaction system.

As shown in table 1 and figure 5, XPS spectra of $\text{Cr } 2p_{3/2}$ for 12.5 wt% $\text{CrO}_x/\text{TiO}_2$ and Al_2O_3 catalysts contain two main peaks at 578.9–579.2 eV for Cr(VI) and 576.3–576.5 eV for Cr(III), respectively [16]. The intensity of Cr(VI) species increase and that of Cr(III) species attributed to the formation of $\alpha\text{-Cr}_2\text{O}_3$ and highly dispersed Cr^{3+} on the catalyst surface decreases as the surface area of TiO_2 and Al_2O_3 increases. The XPS spectra well agrees with the results from XRD for the formation of $\alpha\text{-Cr}_2\text{O}_3$ on the

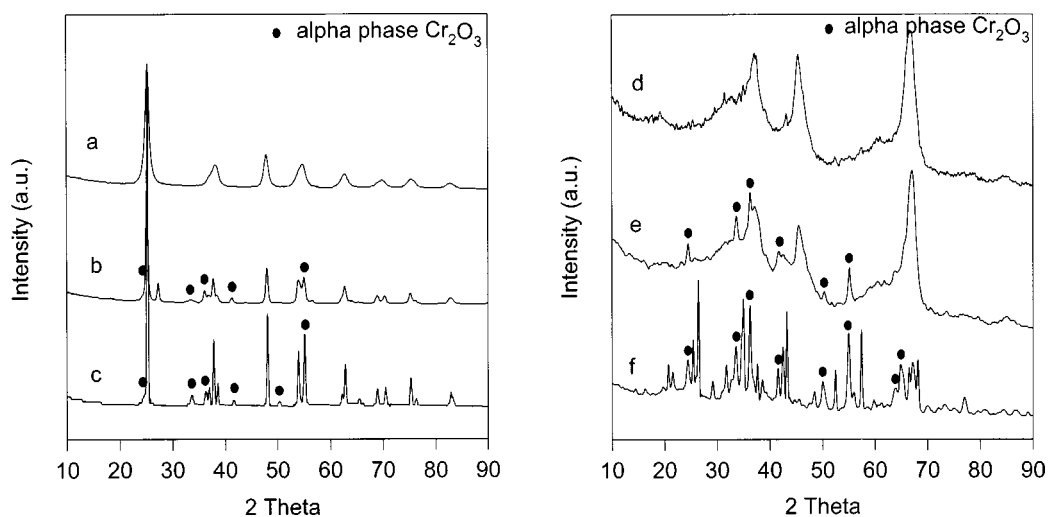


Figure 4. X-ray diffraction patterns of CrO_x catalysts supported on TiO_2 (250 (a), 58 (b) and $17 \text{ m}^2/\text{g}$ (c)) and Al_2O_3 (290 (d), 155 (e) and $25 \text{ m}^2/\text{g}$ (f)).

Table 1
XPS and XRD data for 12.5 wt% CrO_x catalysts supported on TiO_2 and Al_2O_3 containing a variety of catalyst surface areas.

Catalyst ^a	Concentration $\alpha\text{-Cr}_2\text{O}_3^b$ (wt%)	Cr(VI)/Cr(III)	Binding energy Cr $2p_{3/2}$ (eV)	
			Cr(VI)	Cr(III)
$\text{CrO}_x/\text{TiO}_2(250)$	N.D. ^c	50.3/49.7	579.1	576.5
$\text{CrO}_x/\text{TiO}_2(58)$	4.57	32.1/67.9	578.9	576.3
$\text{CrO}_x/\text{TiO}_2(17)$	5.86	27.3/72.7	579.2	576.5
$\text{CrO}_x/\text{Al}_2\text{O}_3(290)$	N.D.	58.0/42.0	579.2	576.5
$\text{CrO}_x/\text{Al}_2\text{O}_3(155)$	3.04	37.0/63.0	579.0	576.5
$\text{CrO}_x/\text{Al}_2\text{O}_3(25)$	7.33	24.0/76.0	579.0	576.3

^a The value in parentheses represents the surface area of TiO_2 and Al_2O_3 .

^b Quantitative XRD data.

^c N.D. = no detection.

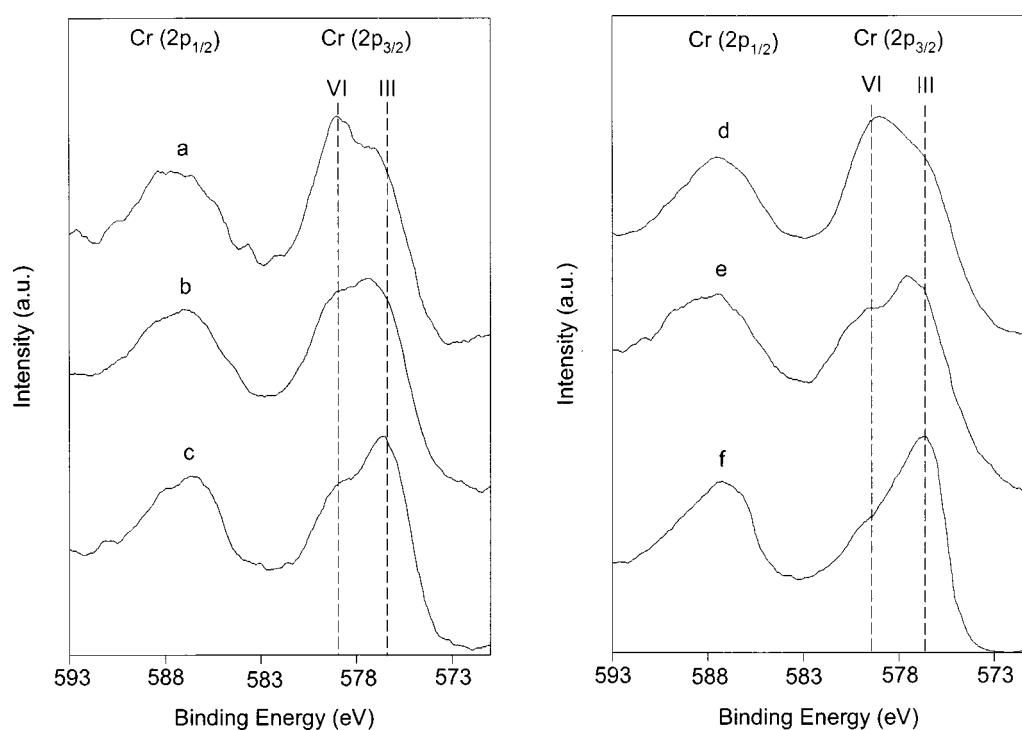


Figure 5. XPS spectra of 12.5 wt% CrO_x catalysts supported on TiO_2 (250 (a), 58 (b) and $17 \text{ m}^2/\text{g}$ (c)) and Al_2O_3 (290 (d), 155 (e) and $25 \text{ m}^2/\text{g}$ (f)).

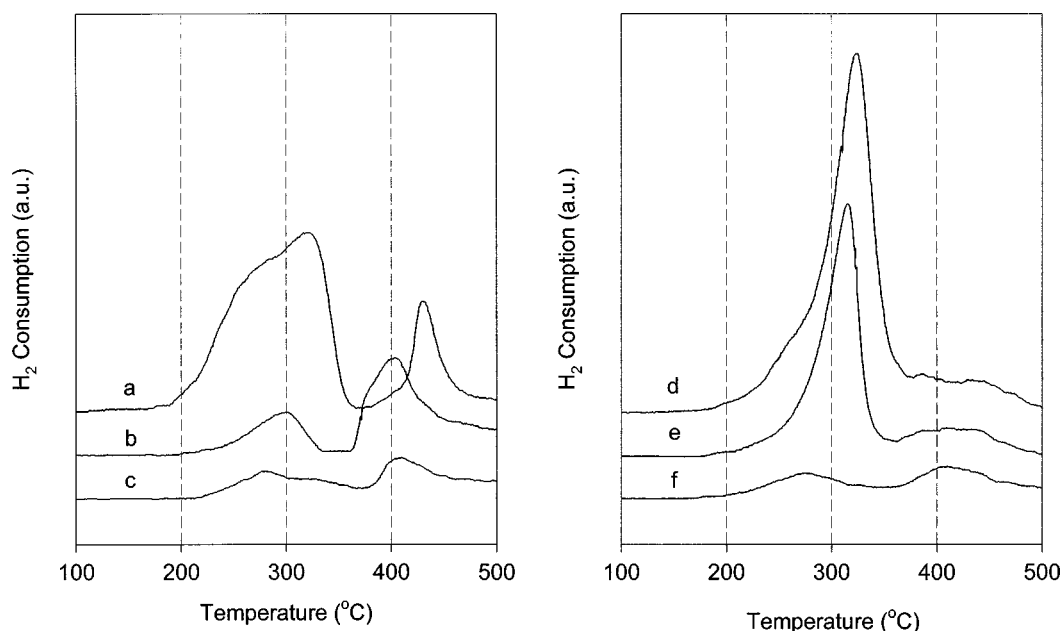


Figure 6. TPR profiles of 12.5 wt% CrO_x catalysts supported on TiO_2 (250 (a), 58 (b) and 17 m^2/g (c)) and Al_2O_3 (290 (d), 155 (e) and 25 m^2/g (f)).

catalyst surface, and they also imply that a high oxidation state of chromium oxide, Cr(VI), is more active than Cr(III) for the PCE removal reaction.

In order to verify the role of Cr(VI) for this reaction system, 12.5 wt% $\text{CrO}_x/\text{Al}_2\text{O}_3$ (290 m^2/g), which was prereduced with H_2 at 450 °C for 3 h, was particularly examined. The PCE removal activity of the prereduced catalyst, 16% of PCE conversion, was much lower than that of the oxidized catalyst, 91%, at 200 °C, and it is gradually improved with respect to the reaction time due to the reoxidation of the prereduced chromium oxide, Cr(III) to Cr(VI), during the course of the reaction, particularly at high reaction temperature. The disappearance and the formation of Cr(VI) on the catalyst surface after prereduction and reaction have been also examined by XPS. Thus, it can be concluded that the high oxidation state of chromium species, Cr(VI), is the active reaction site on the catalyst surface for the removal of PCE.

On the basis of the results from XRD and XPS as discussed, the high surface area TiO_2 catalyst containing 12.5 wt% Cr is the best PCE removal catalyst due to the stabilization of active Cr(VI) and less formation of $\alpha\text{-Cr}_2\text{O}_3$ on the catalyst surface by the strong interaction of Cr on the surface of TiO_2 . However, it is hard to distinguish the difference of PCE removal activity for $\text{CrO}_x/\text{TiO}_2$ and Al_2O_3 catalysts containing a similar surface area only by the formation of Cr(VI) and $\alpha\text{-Cr}_2\text{O}_3$ on the catalyst surface. Note that both catalysts contain similar catalyst surface acidity by NH_3 TPD [23].

Figure 6 shows TPR profiles revealing the redox ability of the catalyst for 12.5 wt% $\text{CrO}_x/\text{TiO}_2$ and Al_2O_3 . The catalysts exhibit two major peaks of H_2 consumption at 275–325 °C (low-temperature peak, LTP) and 405–430 °C (high-temperature peak, HTP), due to the reduction of two distinctive high-valent CrO_x species on the catalyst sur-

Table 2
TPR profiles for 12.5 wt% CrO_x catalysts supported on TiO_2 and Al_2O_3 containing a variety of catalyst surface areas.

Catalyst ^a	T_{max} (°C)		Total H_2 consumption (mmol $\text{H}_2/\text{g}_{\text{cat}}$)
	LTP	HTP	
$\text{CrO}_x/\text{TiO}_2$ (250)	320	430	2.116
$\text{CrO}_x/\text{TiO}_2$ (58)	300	400	1.055
$\text{CrO}_x/\text{TiO}_2$ (17)	277	405	0.585
$\text{CrO}_x/\text{Al}_2\text{O}_3$ (290)	325	–	2.384
$\text{CrO}_x/\text{Al}_2\text{O}_3$ (155)	316	–	1.386
$\text{CrO}_x/\text{Al}_2\text{O}_3$ (25)	275	405	0.591

^a The value in parentheses represents the surface area of TiO_2 and Al_2O_3 .

face [24]. Both LTP and HTP are commonly assigned to TPR peaks for more easily reducible Cr(VI) and less reducible Cr(VI), respectively [24,25]. The shift of LTP towards lower temperatures as the surface area of TiO_2 and Al_2O_3 decreases may indicate the formation of more easily reducible CrO_x species on the catalyst surface [26]. Table 2 gives the total amount of H_2 consumption of CrO_x catalysts by TPR. The amount of H_2 consumption increases as the surface area of TiO_2 and Al_2O_3 increases, indicating that the amount of reducible chromate species increases with increasing surface area of the catalyst. Figure 7 reveals the direct relationship between PCE removal activity and H_2 consumption. This confirms that the active reaction site, Cr(VI), on the catalyst surface plays a critical role for the oxidation of PCE, as discussed earlier with XPS results. However, not all Cr(VI) species on the catalyst surface may contain similar PCE removal activity. This may be due to the difference of the interaction between CrO_x and the catalyst surface. As shown in tables 1 and 2, although $\text{CrO}_x/\text{TiO}_2$ (250 m^2/g) maintains lower surface area and Cr(VI) content than $\text{CrO}_x/\text{Al}_2\text{O}_3$ (290 m^2/g), TiO_2 catalyst shows higher catalytic activity than Al_2O_3 .

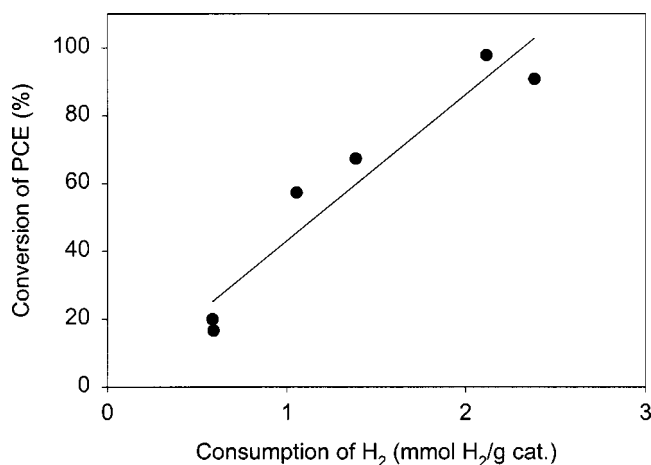


Figure 7. The correlation between PCE removal activity and H_2 consumption of 12.5 wt% CrO_x catalysts supported on TiO_2 ($250 \text{ m}^2/\text{g}$) and Al_2O_3 ($290 \text{ m}^2/\text{g}$).

Wachs and co-workers [17–20] have made an extensive characterization of CrO_x catalysts by laser Raman spectroscopy, and studied the degree of polymerization of Cr(VI) as a function of the surface coverage. Zaki et al. [24] classified Cr(VI) into three groups by TPR, and proposed that the highly reducible chromate at low reduction temperature ($320\text{--}410^\circ\text{C}$) is mainly polymerized Cr(VI) formed on the catalyst surface. TPR profiles shown in figure 6 show that H_2 consumption of $\text{CrO}_x/\text{TiO}_2$ ($250 \text{ m}^2/\text{g}$) shifted towards lower temperature. This reveals that the TiO_2 catalyst contains more easily reducible polymerized chromate species compared to the Al_2O_3 catalyst. The Raman spectra of CrO_x catalysts identify the degree of polymerization of Cr(VI) on the catalyst surface, as shown in figure 8. It should be noted that Cr(III) can be hardly observed by Raman spectroscopy [27]. For $\text{CrO}_x/\text{TiO}_2$ ($250 \text{ m}^2/\text{g}$), the spectral region below 700 cm^{-1} is dominated by the well-known vibrations of the TiO_2 support, and $\sim 800 \text{ cm}^{-1}$ is assigned to anatase [20]. The Raman spectra observed at ~ 860 and $\sim 360 \text{ cm}^{-1}$ for 1 wt% $\text{CrO}_x/\text{Al}_2\text{O}_3$ ($290 \text{ m}^2/\text{g}$) are assigned to the symmetric stretching and bending modes for an isolated tetrahedral surface Cr(VI) oxide species, respectively [18,20,28]. The Raman shifts at ~ 870 and $\sim 995 \text{ cm}^{-1}$ for the 12.5 wt% $\text{CrO}_x/\text{Al}_2\text{O}_3$ ($290 \text{ m}^2/\text{g}$) and $\text{CrO}_x/\text{TiO}_2$ ($250 \text{ m}^2/\text{g}$) catalysts are assigned to the symmetric stretching modes of O--Cr--O for monomeric Cr(VI) , and those of Cr=O bonds for polymeric Cr(VI) oxide species, respectively [29]. The Raman results confirm that the both chromium oxide catalysts possess a polymeric and monomeric chromium oxide species on the catalyst surface depending upon the content of CrO_x and the type of the supports. It is also in agreement with the TPR results shown in figure 6. The formation of the polymerized Cr(VI) can be observed even at the Cr content of 1 wt% for the $\text{CrO}_x/\text{TiO}_2$ ($250 \text{ m}^2/\text{g}$) catalyst. However, no polymeric Cr(VI) can be found for the 1 wt% $\text{CrO}_x/\text{Al}_2\text{O}_3$ ($290 \text{ m}^2/\text{g}$) catalyst. It simply reveals the interaction between CrO_x and catalyst supports, as discussed before. Based upon TPR and Ra-

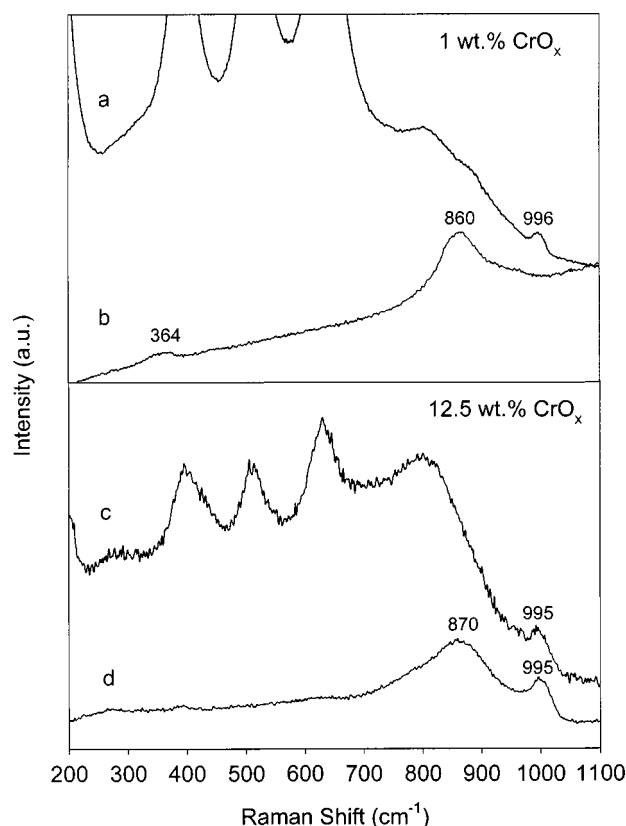


Figure 8. Raman spectra of CrO_x catalysts supported on TiO_2 ($250 \text{ m}^2/\text{g}$) (a, c) and Al_2O_3 ($290 \text{ m}^2/\text{g}$) (b, d).

man results, it can be concluded that the content of Cr(VI) species and their degree of polymerization are critical for the high performance of the PCE decomposition reaction on CrO_x catalysts.

4. Conclusions

The PCE removal activity over chromium oxide catalysts was strongly influenced by the state of chromium oxide phase on the catalyst surface. The high oxidation state of Cr(VI) species was more active than the reduced Cr(III) and crystalline $\alpha\text{-Cr}_2\text{O}_3$ for the oxidation of PCE. The type of supports and their surface areas were critical for the formation of Cr(VI) on the catalyst surface. The 12.5 wt% $\text{CrO}_x/\text{TiO}_2$ containing a high surface area, $250 \text{ m}^2/\text{g}$, is the most active catalyst among the catalysts examined in the present study due to the formation of Cr(VI) , which is the active reaction site for the oxidation of PCE. The degree of polymerization of CrO_x on the catalyst surface may be another aspect for the high performance of the present catalytic reaction system.

References

- [1] J.J. Spivey, Ind. Eng. Chem. Res. 26 (1987) 2165.
- [2] G.C. Bond and N. Sadeghi, J. Appl. Chem. Biotechnol. 25 (1975) 241.

- [3] J.C. Lou and S.S. Lee, *Appl. Catal. B* 12 (1997) 111.
- [4] M.P. Manning, *Hazard. Waste* 1 (1984) 41.
- [5] J.K. Musick and F.W. Williams, *Ind. Eng. Chem. Prod. Res. Dev.* 13 (1974) 175.
- [6] S. Chatterjee and H.L. Greene, *J. Catal.* 130 (1991) 76.
- [7] S. Imamura, H. Tarumoto and S. Ishida, *Ind. Eng. Chem. Res.* 28 (1989) 1449.
- [8] S.C. Petrosius, R.S. Drago, V. Young and G.C. Grunewald, *J. Am. Chem. Soc.* 115 (1993) 6131.
- [9] L. Storaro, R. Ganzerla, M. Lenarda, R. Zaroni, A.J. Lopez, P.O. Pastor and E.R. Castellon, *J. Mol. Catal. A* 115 (1997) 329.
- [10] C.-W. Hong, M.H. Kim, I.-S. Nam and Y.G. Kim, *Hwahak Konghak (J. Korean Institute Chem. Engin.)* 36 (1998) 206.
- [11] K. Ramanathan and J.J. Spivey, *Combust. Sci. Technol.* 63 (1989) 247.
- [12] S.K. Agarwal and J.J. Spivey, *Appl. Catal. A* 82 (1992) 259.
- [13] S. Kawi and M. Te, *Catal. Today* 44 (1998) 101.
- [14] X.-Z. Jiang, L.-Q. Zhang, X.-H. Wu and L. Zheng, *Appl. Catal. B* 9 (1996) 229.
- [15] R.M. Lago, M.L.H. Green, S.C. Tsang and M. Odlyha, *Appl. Catal. B* 8 (1996) 107.
- [16] P.W. Park and J.S. Ledford, *Langmuir* 13 (1997) 2726.
- [17] D.S. Kim, J.-M. Tatibouet and I.E. Wachs, *J. Catal.* 136 (1992) 209.
- [18] B.M. Weckhuysen, I.E. Wachs and R.A. Schoonheydt, *Chem. Rev.* 96 (1996) 3327.
- [19] M.A. Vuurman, F.D. Hardcastle and I.E. Wachs, *J. Mol. Catal.* 80 (1993) 209.
- [20] F.D. Hardcastle and I.E. Wachs, *J. Mol. Catal.* 46 (1988) 173.
- [21] M.I. Zaki, N.E. Fouad, J. Leyer and H. Knözinger, *Appl. Catal.* 21 (1986) 359.
- [22] F. Cavani, M. Koutyrev, F. Trifiro, A. Bartolini, D. Ghisletti, R. Iezzi, A. Santucci and G. Del Piero, *J. Catal.* 158 (1996) 236.
- [23] S.D. Yim, M.S. Thesis, Postech (Korea) (1998).
- [24] M.I. Zaki, N.E. Fouad, G.C. Bond and S.F. Tahir, *Thermochim. Acta* 285 (1996) 167.
- [25] B. Parlitz, W. Hanke, R. Fricke, M. Richter, U. Roost and G. Öhlmann, *J. Catal.* 94 (1985) 24.
- [26] B.M. Weckhuysen, R.A. Schoonheydt, J.-M. Jehng, I.E. Wachs, S.J. Cho, R. Ryoo, S. Kijlstra and E. Poels, *J. Chem. Soc. Faraday Trans.* 91 (1995) 3245.
- [27] M.A. Vuurman, D.J. Stufkens, A. Oskam, J.A. Moulijn and F. Kapteijn, *J. Mol. Catal.* 60 (1990) 83.
- [28] D.H. Cho, S.D. Yim, G.H. Cha, J.S. Lee, Y.G. Kim, J.S. Chung and I.-S. Nam, *J. Phys. Chem. A* 102 (1998) 7913.
- [29] O.F. Gorris and L.E. Cadús, *Appl. Catal. A* 180 (1999) 247.